

First principles computer simulations of $\text{Li}_{10}\text{GeP}_2\text{S}_{12}$ and related lithium superionic conductors

N. A. W. Holzwarth

Department of Physics, Wake Forest University, Winston-Salem, NC, 27109, USA

Introduction

A recent paper by Kamaya *et al.* [1] reported a new crystalline superionic conductor having a compact tetrahedral structure and a stoichiometry of $\text{Li}_{10}\text{GeP}_2\text{S}_{12}$. The room temperature conductivity was reported to be 0.01 S/cm, comparable to liquid electrolyte conductivities and five times higher the compositionally related thio-LISICON material $\text{Li}_{3.25}\text{Ge}_{0.25}\text{P}_{0.75}\text{S}_4$ developed earlier, [2] and twice as high as the lithium thiophosphate ceramic material $\text{Li}_7\text{P}_3\text{S}_{11}$ [3]. The survey of electrolyte results presented in Ref. 1 is reproduced in Fig. 1. Because of its potential technological importance, several research groups have already published simulation results on this material [4-5]. This poster presents a progress report on our contributions to the effort to understand some of the fundamental properties of $\text{Li}_{10}\text{GeP}_2\text{S}_{12}$ and a hypothetical analog: $\text{Li}_{10}\text{SiP}_2\text{S}_{12}$.

Computational Methods

The computational methods used in this work were the same as those used in our previous studies of Li phosphate and thiophosphate electrolytes and related materials [6-8]. Briefly, we used density functional theory [9] with the local density approximation (LDA) [10] to treat the electronic states and the Born-Oppenheimer approximation to treat the atomic positions $\{\mathbf{R}^a\}$, resulting in a determination of the “total energy” $E(\{\mathbf{R}^a\})$, or zero temperature internal energy, of the system. Most of the computations were carried out using the *PWscf* package; [11] while a few calculations were performed using the *abinit* [12] and *pwpaw* [13] packages as well. Visualizations were constructed using the *OpenDX* [14] and *XCrySDEN* [15] software packages.

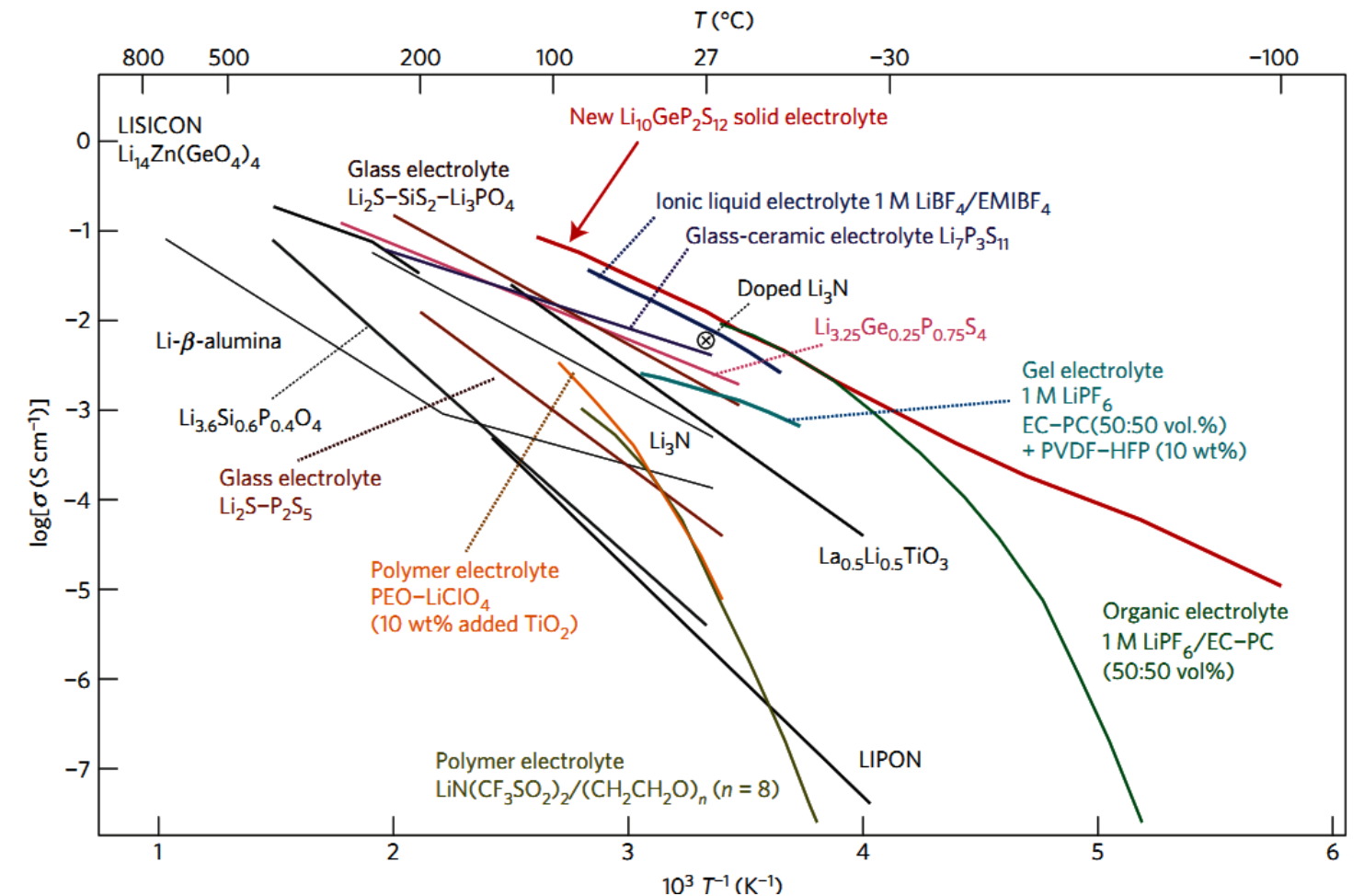


FIG. 1: Figure reproduced from Ref. [1] showing conductivities of various electrolytes as a function of temperature.

Starting from experimental information, restricted optimization of the total energy $E(\{\mathbf{R}^a\})$ with respect to the atomic positions $\{\mathbf{R}^a\}$ and unit cell parameters, allows us to model stable and meta-stable structures. In addition to geometric information we can determine relative energies and estimate the enthalpy of formation ΔH . In addition, migration energies (E_m) for Li ion migration were estimated using the “nudged elastic band” method. [16]

Constituents of $\text{Li}_{10}\text{GeP}_2\text{S}_{12}$

The crystal structures of components of $\text{Li}_{10}\text{GeP}_2\text{S}_{12}$ have been characterized experimentally: Li_3PS_4 [17] and Li_4GeS_4 [18] and Li_4SiS_4 [19]. Li_3PS_4 has been found to form 3 crystal structures; the low temperature structure, labeled $\gamma\text{-Li}_3\text{PS}_4$ in Ref. [17], having $Pmn2_1$ symmetry, has the lowest energy according to our calculations as shown in Fig. 3. The other two structures shown in this figure are the lowest energy ordered structures consistent with the experimental data. The structure of Li_4GeS_4 having $Pmna$ symmetry (Ref. 18) is shown in Fig. 2. For simplicity we assume Li_4SiS_4 to have the same structure. The calculated heats of formation are given in units of eV/formula unit.

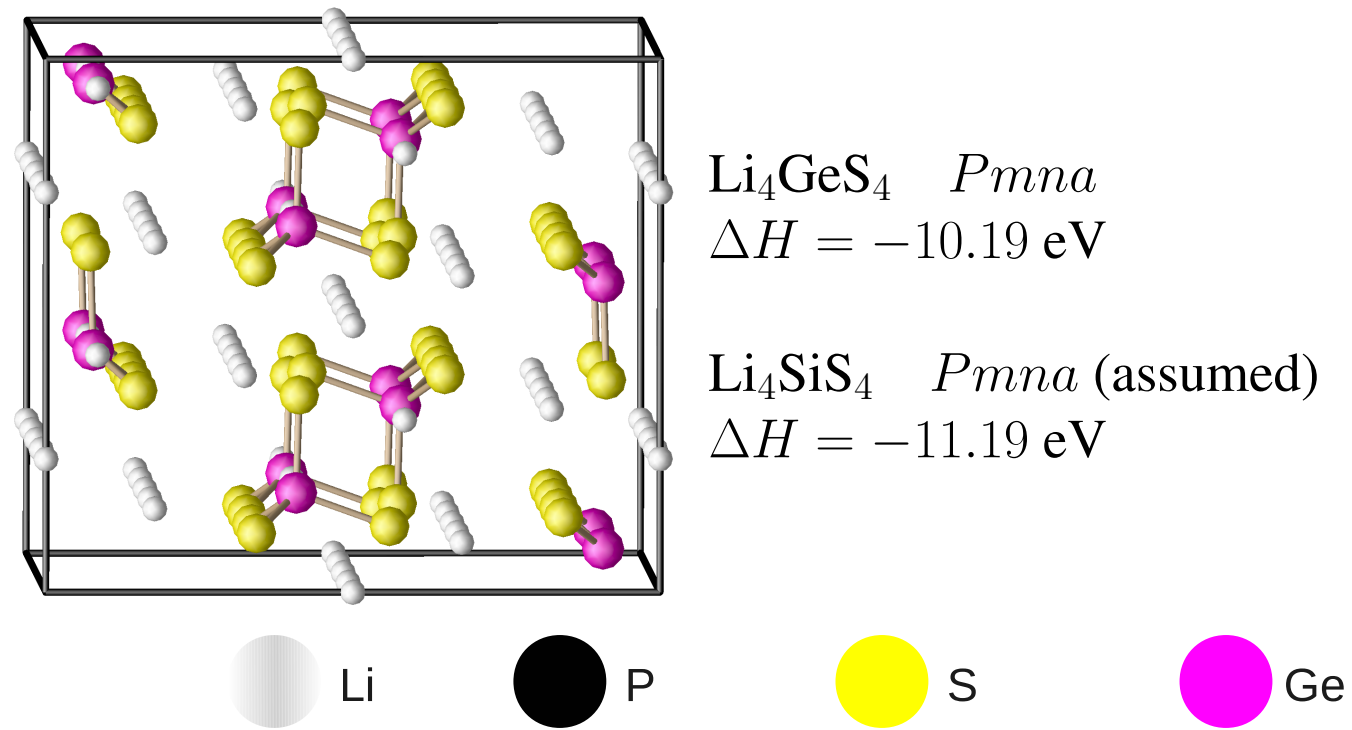
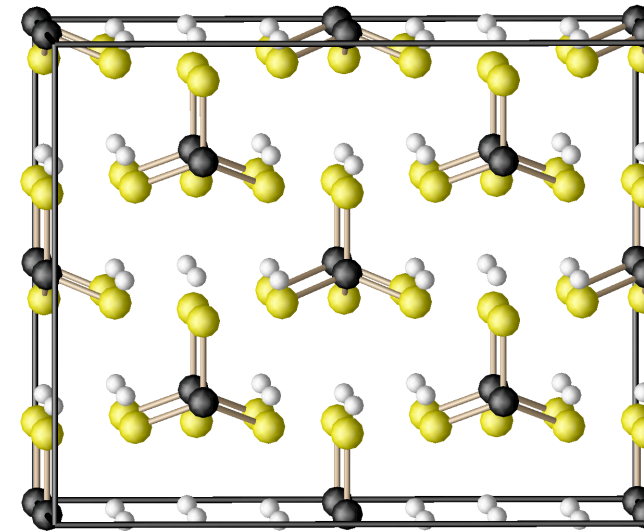
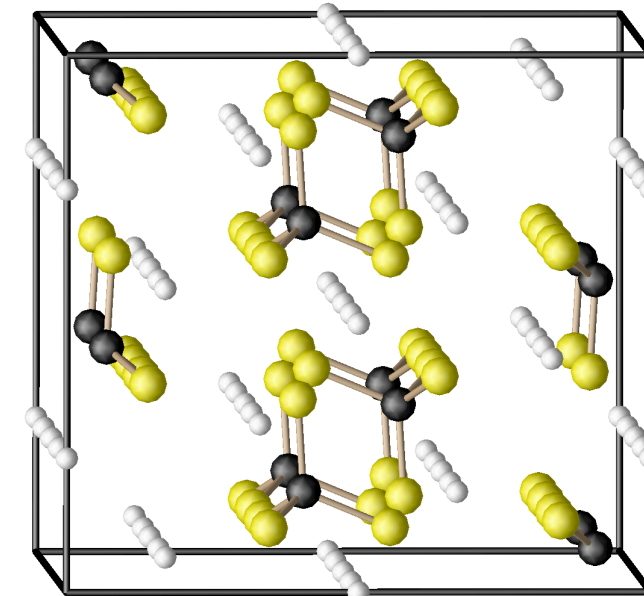


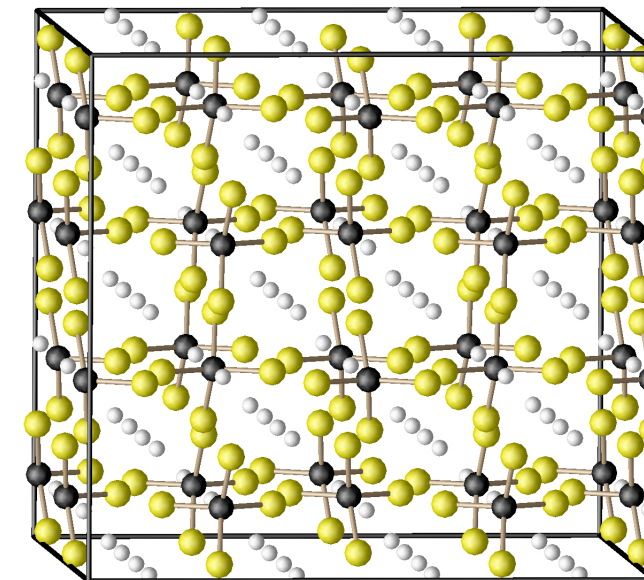
FIG 2: Optimized structure of Li_4GeS_4 using the structure of Ref. [18], listing calculated heats of formation of both Li_4GeS_4 and Li_4SiS_4 in this structure.



$\gamma\text{-Li}_3\text{PS}_4$ $Pmn2_1$
 $\Delta H = -8.36$ eV



$\beta\text{-Li}_3\text{PS}_4$ $Pnma$
 $\Delta H = -8.28$ eV



$\alpha\text{-Li}_3\text{PS}_4$ $Pbcn$
 $\Delta H = -8.12$ eV

FIG 3: Optimized structures of Li_3PS_4 based on structures of Ref. [17], listing calculated heats of formation of lowest energy forms.

Optimized structure of $\text{Li}_{10}\text{GeP}_2\text{S}_{12}$

The calculated optimized structure of $\text{Li}_{10}\text{GeP}_2\text{S}_{12}$ is shown in Figs. 4 and 5. The calculated heat of formation for this structure is $\Delta H = 26.15$ eV/formula unit. The optimized structure for $\text{Li}_{10}\text{SiP}_2\text{S}_{12}$ looks similar and its calculated heat of formation is $\Delta H = 27.18$ eV/formula unit.

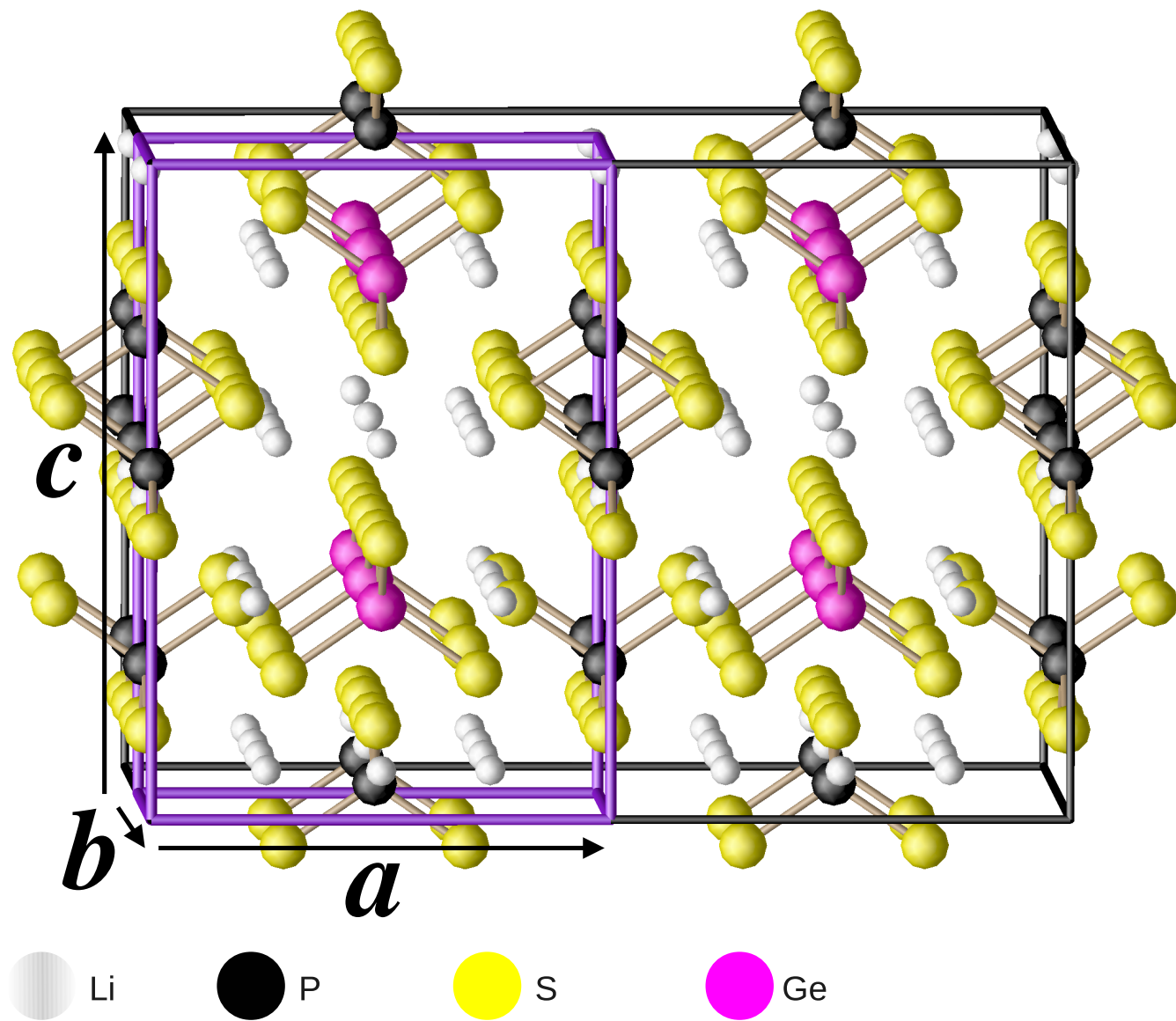


FIG 4: Optimized structure of $\text{Li}_{10}\text{GeP}_2\text{S}_{12}$ shown in a projection in the **a-c** plane.

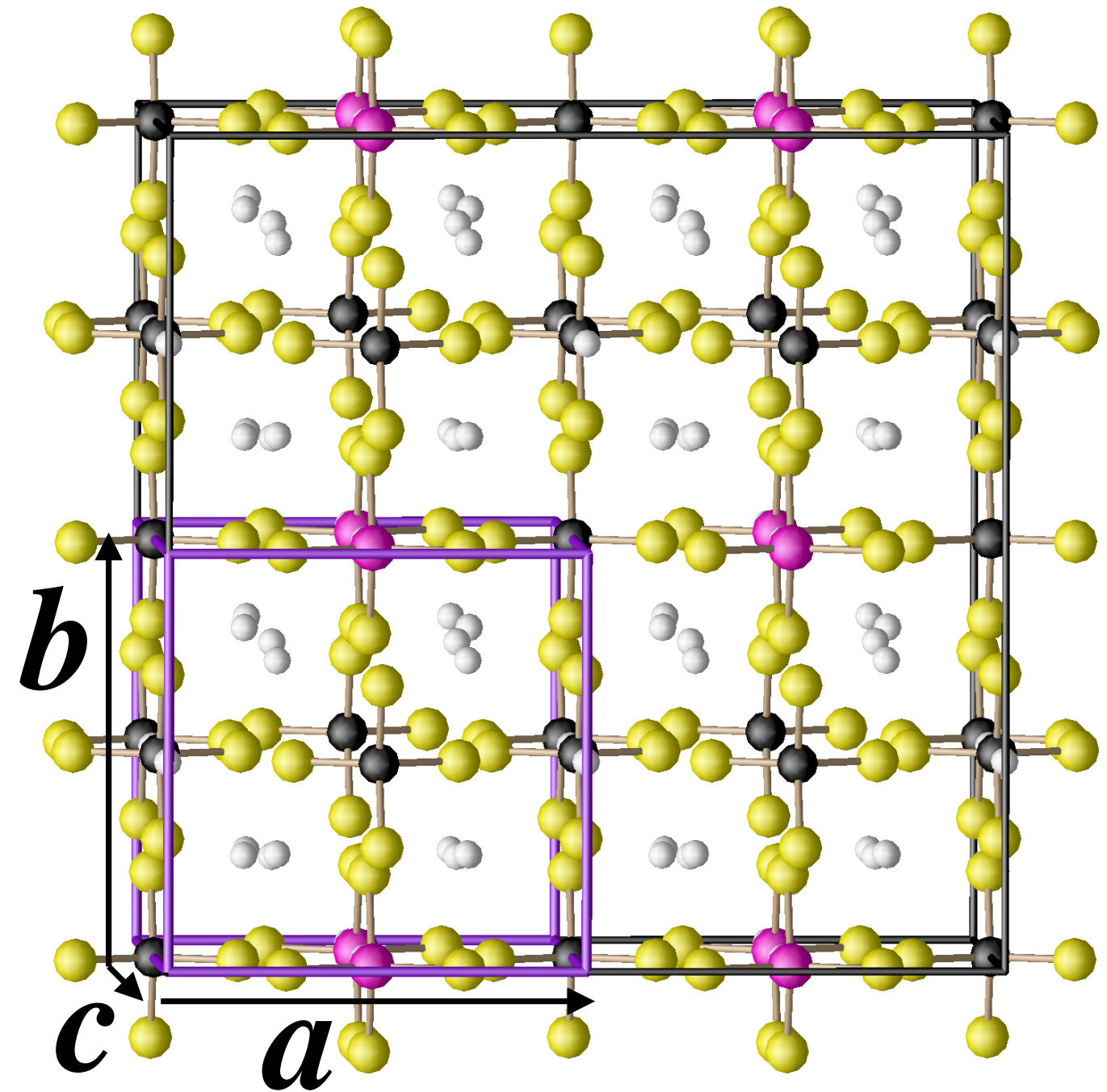


FIG 5: Optimized structure of $\text{Li}_{10}\text{GeP}_2\text{S}_{12}$ shown in a projection in the **a-b** plane.

Details of structural optimization

The experimentally determined structure found in Ref. [1] has space group $P4_2/nmc$ (#137) with some sites fractionally occupied. We searched for compatible ideal structures, finding the greatest energetic sensitivity in the placement of P and Ge sites and finding the most stable structure to have an energy more than 0.5 eV/formula unit lower than any of the others. With the help of the program FINDSYM [20], we found the space group symmetry of the lowest energy ideal structure to be $P4_2mc$ (#105) with the fractional coordinate relationship $(x, y, z) \rightarrow (y, x, -z)$ for #137 \rightarrow #105. Table 1 below shows the correspondances of the inequivalent fractional lattice coordinates.

Experiment structure:
 Space group $P4_2/nmc$ (#137)

Atom	g	x	y	z
Li(1) 16h	0.69	0.26	0.27	0.18
Li(2) 4d	1.00	0.00	0.50	0.94
Li(3) 8f	0.64	0.25	0.25	0.00
Ge(1) 4d	0.52	0.00	0.50	0.69
P(1) 4d	0.49	0.00	0.50	0.69
Ge(2) 2b	0.00	0.00	0.00	0.50
P(2) 2b	1.00	0.00	0.00	0.50
S(1) 8g	1.00	0.00	0.18	0.41
S(2) 8g	1.00	0.00	0.30	0.10
S(3) 8g	1.00	0.00	0.70	0.79

Calculated structure:
 Space group $P4_2mc$ (#105)*

Atom	g	x	y	z
Li(1) 8f	1.00	0.23	0.23	0.29
Li(2) 2a/2b	1.00	0.00	0.50	0.94
Li(3) 8f	1.00	0.26	0.22	0.03
Ge(1) 2b	1.00	0.50	0.00	0.79
P(1) 2a	1.00	0.00	0.50	0.68
P(2) 2c	1.00	0.00	0.00	0.50
S(1) 4d/4e	1.00	0.00	0.20	0.41
S(2) 4d/4e	1.00	0.00	0.30	0.09
S(3) 4d/4e	1.00	0.00	0.70	0.78

*Wyckoff symbols for #105, coordinates in #137 convention.

TABLE 1: Comparison of structures for $\text{Li}_{10}\text{GeP}_2\text{S}_{12}$ in the experimental structure (#137) with fractionally occupied sites and the related ideal structure (#105).

Lattice Parameters

The lattice parameters calculated for the idealized structures of $\text{Li}_{10}\text{GeP}_2\text{S}_{12}$ and $\text{Li}_{10}\text{SiP}_2\text{S}_{12}$ are listed in Table 2. The fact that calculated lattice constants are smaller than experiment is consistent with known systematic errors in LDA calculations, although relative sizes are expected to be modeled correctly. It is interesting that Ge and Si materials are predicted to have very similar lattice parameters.

	a (Å)	c (Å)
$\text{Li}_{10}\text{GeP}_2\text{S}_{12}$ (exp*)	8.72	12.63
$\text{Li}_{10}\text{GeP}_2\text{S}_{12}$ (calc)	8.56	12.23
$\text{Li}_{10}\text{SiP}_2\text{S}_{12}$ (calc)	8.55	12.16

*Ref. [1]

TABLE 2: Experimental and calculated lattice parameters.

Predicted decomposition reactions

Table 3 summarizes some of the calculated energy relationships among the electrolytes that we have studied. Interestingly, all of the materials studied so far are predicted to be *unstable* relative to decomposition into their constituents.

	ΔH (eV)
$\text{Li}_{10}\text{GeP}_2\text{S}_{12} \rightarrow 2\text{Li}_3\text{PS}_4 + \text{Li}_4\text{GeS}_4$	0.77
$\text{Li}_{10}\text{SiP}_2\text{S}_{12} \rightarrow 2\text{Li}_3\text{PS}_4 + \text{Li}_4\text{SiS}_4$	0.74
$\text{Li}_{13}\text{GeP}_3\text{S}_{16} \rightarrow 3\text{Li}_3\text{PS}_4 + \text{Li}_4\text{GeS}_4$	0.55
$\text{Li}_{13}\text{SiP}_3\text{S}_{16} \rightarrow 3\text{Li}_3\text{PS}_4 + \text{Li}_4\text{SiS}_4$	0.62

TABLE 3: Reactions predicted from calculated enthalpy of formation energies (at zero temperature).

Analysis of Li ion migration

So far, we have studied the migration of Li ion vacancies in a 2x2x1 supercell using the NEB [16] approach. The distinct Li sites (labeled ①, ②, and ③, according to the regular crystallographical analysis) are shown in Fig. 6 in a **a** - **c** axis projection. The corresponding relative energies of the vacancy sites are listed in Table 4.

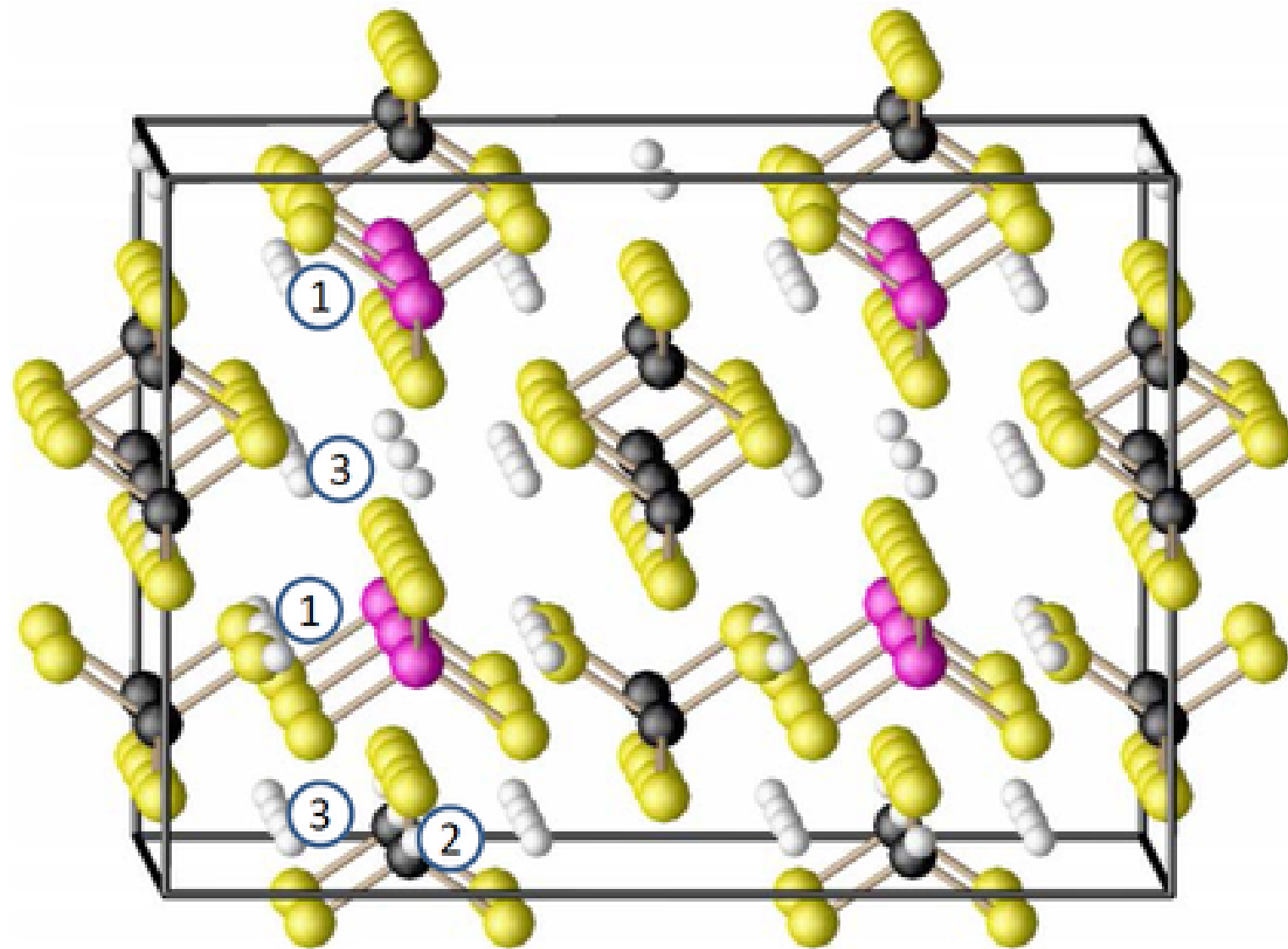


FIG 6: Structural diagram of $\text{Li}_{10}\text{GeP}_2\text{S}_{12}$ indicating Li vacancy sites.

Relative vacancy energies

Vacancy site	$\text{Li}_{10}\text{SiP}_2\text{S}_{12}$	$\text{Li}_{10}\text{GeP}_2\text{S}_{12}$
①	0.04	0.00
②	0.67	0.52
③	0.00	0.11

TABLE 4: Energies of relaxed vacancies in 2x2x1 supercell relative to the lowest energy site in eV units – ③ for $\text{Li}_{10}\text{SiP}_2\text{S}_{12}$ and ① for $\text{Li}_{10}\text{GeP}_2\text{S}_{12}$.

Energy paths for vacancy migration

The NEB results for Li ion vacancy migration are shown in Fig. 7. They suggest that for $\text{Li}_{10}\text{SiP}_2\text{S}_{12}$, vacancy migration along the **c**- axis with the ① and ③ sites has a barrier of $E_m = 0.5$ eV while migration including the ② site is energetically unfavorable. On the other hand for $\text{Li}_{10}\text{GeP}_2\text{S}_{12}$ the vacancy migration barrier is approximately $E_m = 0.5$ eV for path segments including both the **c**- and **a**- axes.

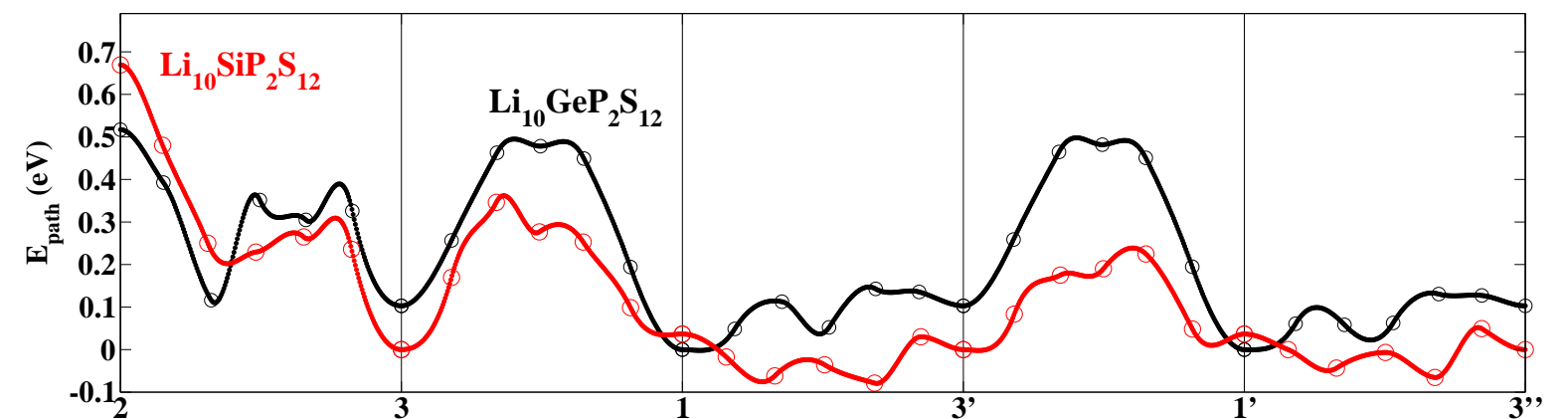


FIG 7: Energy path diagram for Li ion vacancy migration in $\text{Li}_{10}\text{SiP}_2\text{S}_{12}$ (red) and $\text{Li}_{10}\text{GeP}_2\text{S}_{12}$ (black).

Summary and Conclusions

We have found meta-stable structures for both $\text{Li}_{10}\text{GeP}_2\text{S}_{12}$ and $\text{Li}_{10}\text{SiP}_2\text{S}_{12}$. The lowest energy ordered structure has space group $P4_2mc$ instead of the experimental structure with partial occupancies and space group $P4_2/nmc$. The fact that even the idealized structure is unstable relative to decomposition into the constituent compounds, presents a challenge to the theory. Specifically, if we assume that the energetics are reasonably accurate, we are challenged to explain how the materials can be physically realized, within the framework of equilibrium thermodynamics or kinetic theories.

Our preliminary studies of Li ion vacancy migration find $E_m \approx 0.5$ eV for both $\text{Li}_{10}\text{GeP}_2\text{S}_{12}$ and $\text{Li}_{10}\text{SiP}_2\text{S}_{12}$ with slightly different details. The fact that this result is approximately twice the activation energy found in experiment [1] suggests that pure vacancy migration in these materials is not the dominant conduction mechanism.

Acknowledgements

This work was supported by NSF grant DMR-1105485 and by the Wake Forest University DEAC computer cluster.

Bibliography

- [1] N. Kamaya, K. Homma, Y. Yamakawa, M. Hirayama, R. Kanno, M. Yonemura, T. Kamiyama, Y. Kato, S. Hama, K. Kawamoto, and A. Mitsui *Nature Materials* **10**, 682 (2011).
- [2] R. Kanno and M. Murayama, *J. Electrochem. Soc.* **48**, A742 (2010).
- [3] A. Hayashi, K. Minami, S. Ujiie, and M. Tatsumisago *J. Non-crystalline Solids* **356** 2670, (2010).
- [4] S. Adams and R. P. Rao, *J. Mater. Chem* **22**, 7687 (2012).
- [5] Y. Mo, S. P. Ong, and G. Ceder, *J. Mater. Chem* **24**, 15 (2012).
- [6] Y. A. Du and N. A. W. Holzwarth, *J. Electrochem. Soc.* **154**, A999 (2007); Y. A. Du and N. A. W. Holzwarth, *Phys. Rev. B* **81**, 184106 (2010).
- [7] N. A. W. Holzwarth, *J. Power Sources* **196** 6870 (2011).
- [8] N. D. Lepley and N. A. W. Holzwarth, *J. Electrochem. Soc.* **59** A538 (2012).
- [9] P. Hohenberg, W. Kohn, *Physical Review* **136**, B864 (1964); W. Kohn, L. J. Sham, *Physical Review* **140**, A1133 (1965).
- [10] J. P. Perdew, Y. Wang, *Phys. Rev. B* **45**, 13244 (1992).
- [11] P. Giannozzi, et al., *J. Phys.: Condens. Matter* **21**, 394402 (19pp) (2009). Available from the website <http://www.quantum-espresso.org>.
- [12] X. Gonze, et al., *Computer Physics Communications* **180**, 2582 (2009). Available from the website <http://www.abinit.org>.
- [13] A. R. Tackett, N. A. W. Holzwarth, G. E. Matthews, *Computer Physics Communications* **135**, 348 (2001). Available from the website <http://pwpaw.wfu.edu>.
- [14] OpenDX The Open Source Software Project Based on IBMs Visualization Data Explorer is available from the web site <http://www.opendx.org>.
- [15] A. Kokalj, *Journal of Molecular Graphics and Modelling* **17**, 176 (1999).
- [16] H. Jónsson, G. Mills, K. W. Jacobsen, *Classical and Quantum Dynamics in Condensed Phase Simulations*, B. J. Berne, G. Ciccotti, D. F. Coker, eds. (World Scientific, Singapore, 1998), pp. 385404; G. Henkelman, B. P. Uberuaga, H. Jónsson, *J. Chem. Phys.* **113**, 9901 (2000); G. Henkelman, H. Jónsson, *J. Chem. Phys.* **113**, 9978 (2000).
- [17] K. Homma, M. Yonemura, T. Kobayashi, M. Nagao, M. Miryama, and R. Kanno, *Solid State Ionics* **182** 53 (2011).
- [18] M. Murayama, R. Kanno, Y. Kawamoto, and T. Kamiyama, *Solid State Ionics* **154-155** 789 (2002).
- [19] M. Murayama, R. Kanno, M. Irie, S. Ito, T. Hata, N. Sonoyama, and Y. Kawamoto, *J. Solid State Chem.* **168** 140 (2002).
- [20] FINDSYM was written by Stokes, Campbell, and Hatch at Brigham Young University (<http://stokes.byu.edu/iso/>).